^{100}Mo(p⃗,d)^{99}Mo reaction at 50 MeV and direct reaction analysis

F. Aramaki[a], Syafarudin[b], G. Wakabayashi[b], Y. Uozumi[b], N. Ikeda[b]
M. Matoba[b], T. Sakae[c], N. Koori[d]

[a] Kyushu Institute of Information Science
[b] Dept. of Nuclear Engineering, Kyushu University
[c] Proton Medical Research Center, Tsukuba University
[d] College of General Education, University of Tokushima

The ^{100}Mo($\vec{p}$,d)^{99}Mo reaction has been studied with 50 MeV polarized protons. Angular distribution of the differential cross section and the analyzing power have been measured for neutron hole states in the ^{99}Mo up to the excitation energy of 6 MeV. The data analysis with a standard distorted-wave Born Approximation (DWBA) theory provides transferred angular momenta(l and j) and spectroscopic factors of neutron hole states for 40 excited states from the ground states up to the excitation energy of 3 MeV. The direct reaction model and the continuous strength functions were used to analyze spectrum regions from discrete levels to continuum.

I. Introduction

By means of medium-weight mass target nuclei and moderate bombarding energy, one can observe many discrete excitation levels and just above them a continuum spectrum in the one-nucleon transfer reactions. As shown in Figure 1, the spectrum is structured discretely and gradually becomes structureless in the higher area, and finally forms a plateau.[1, 2, 3] As for the discrete region, exprimental data for assigning lj-values for excitation levels are scarce, and assignment results are not in good agreement, especilly abeve 2MeV. In this paper, we describe the new results in assigning lj-values using ^{100}Mo($\vec{p}$,d)^{99}Mo reaction at 50MeV.

Continuum spectrum is undestood as a reflection of the phenomena occured in shell-orbit, e.g. nuclear dumping, shell-orbit fragmentation, nuclear surface vibration. The effect of nucleon pickup and direct reaction plays an important role more contributive than other effects. An approach proposed by Lewis[4] is employed based on DWBA and asymmetrical Lorentzian form atrength function having energy dependent spreading width.[5, 6]

This paper describes results of studies on ^{100}Mo($\vec{p}$,d)^{99}Mo reaction with 50MeV polarized protons. Assignment of excitation levels below 4MeV region was carried out and compared the derived value with previously observed values, and spectrum was analyzed using a continuous strength function and DWBA-based cross sections of the corelated neutron hole states.

II. Experiment

The experiment was carried out at the AVF cyclotron facility of the Research Center for Nuclear Physics, Osaka University,using the enriched (97.27%) ^{100}Mo target foil. The beams of high energy resolution (∼30keV) and a polarized proton beam with the polarization of about 80% accelarated to the energy of 50MeV was used. Polarized beam data determined the spin parity values more definitely. Emitted dueterons from ^{100}Mo($\vec{p}$,d)^{99}Mo reaction were detected and momentum analyzed by the focal plane of a RAIDEN spectrograph with a position sensitive proportional counter detector system. Angular distributions of cross sections and analyzing powers were detected at 8 °∼43 °laboratory angles. The measured

energy range coresponds to the excitation energy region from the ground state to about 6.5 MeV. Details of the expriment procedure are described in the previous papers.[5, 7]

Fourty one levels were analyzed in the excitaion energy below 4 MeV. From comparisons between the exprimental angular distribution of the cross sections and the predictions of the DWBA theory using the optical potential parameters, the lj–angular momentum transfer were assigned. The normalization of the cross section was performed by the scaling the measured ^{100}Mo(p,p) elastic scattering cross section to an optical model predictions using the parameters of global potential.

Figure1 shows a typical double differential cross section for the ^{100}Mo($\vec{p}$,d)^{99}Mo reaction at the 8 °laboratory angle. From the comparisons between the exprimental and theoretical angular distributions of cross sections and analyzing powers, the lj-angular momentum transfers were assigned. Thirty six levels were abnalyzed in the excitation energy region below 3.5MeV and the lj-transfers were assigned for 36 levels.

For the continuum area, double differential cross sections are predicted by the DWBA using global optical potential. The double differential cross section-energy spectra were reproduced fairly well using the DWBA-based cross sections and the asymmetrical Lorentzian form strength response function having energy–dependent spreading width. The absolute values are in good agreement and very close order to the exprimental data.

III. Theoretical Analysis

Double differntial cross sections are analyzed with the direct reaction model composed by an incoherent sum of the DWBA predictions from all the constituent shell-orbits, as expressed by,

$$\frac{d\sigma}{d\Omega}(E) = 2.30 \sum_{l,j} \left[\frac{C^2 S_{l,j}(E)}{2j+1} \times \left(\frac{d\sigma}{d\Omega}^{DW}_{l,j}(E) \right) \right] \qquad (1)$$

where $d\sigma/d\Omega|^{DW}_{l,j}(E)$ is the DWBA cross section, $C^2S_{l,j}(E)$ is the strength function of spectroscopic factor for the $lj-$transfer, given as follows,

$$C^2 S_{l,j}(E) = \left(\sum_{l,j} C^2 S_{l,j} \right) \times f_{l,j}(E) \qquad (2)$$

The degrees of continuum strength is estimated by the Breit-Wigner form,

$$f_{l,j}(E) = \frac{n_0}{2\pi} \frac{\Gamma(E)}{(|E - E_F| - E_{l,j})^2 + \Gamma^2(E)/4} \qquad (3)$$

where E_{ij} is the the calculated energy of the single-particle state which varies with the spreading width $\Gamma(E)$, and n_0 is the renormalization constant and E_R the resonance energy. The spreading widths $\Gamma(E)$ are expressed with the function proposed by Mahaux and Sartor [8] and Brown and Rho as follows[9]

$$\Gamma(E) = \frac{\epsilon_0 (E - E_F)^2}{(E - E_F)^2 + E_0^2} + \frac{\epsilon_1 (E - E_F)^2}{(E - E_F)^2 + E_1^2} \qquad (4)$$

where ϵ_0, ϵ_1, E_0, and E_1 are constants used to express the effect of nuclear damping. The used parameter values are as follows,

$$\begin{array}{ll} \epsilon_0 = 19.4 \text{ (MeV)}, & E_0 = 18.4 \text{ (MeV)}, \\ \epsilon_1 = 1.40 \text{ (MeV)}, & E_1 = 1.60 \text{ (MeV)} \end{array} \qquad (5)$$

The sum-rules of the spectroscopic factors of neutron orbits for $T \pm \frac{1}{2}$ isospin states above the closed shell core are estimated with a simple shell model prescription as described in the following equation[10]

$$\sum C^2 S = \begin{cases} n_n - \dfrac{n_p}{2T+1} & \text{for} \quad T_< = T - \frac{1}{2} \\ \dfrac{n_p}{2T+1} & \text{for} \quad T_> = T + \frac{1}{2} \end{cases} \qquad (6)$$

where n_n and n_p are the numbers of neutrons and protons, respectively, above the closed shell core and T is the target isospin.

The differential cross section and analyzing power data were analyzed with the DWBA code DWUCK[11] based on the zero-range and local energy appoximation model.

IV. Discussion

Angular distributions of cross sections and analyzing powers for 36 levels assigned for laboratory angles from 8 °∼43 °. Results are

shown in table 1 along with DWBA prediction at 8 ° laboratory angle. The measured energy spectrum of double differential cross section and analyzing powers were coverted to 500keV wide energy spectra. In Figures 2 and 3, solid lines represents theoretical differential cross section and analyzing powers, and histograms the experimental ones. Not only for 8 °, the theory predicts differential cross section in discrete region(～3MeV) fairly well, but in the region above 4MeV it does not and differential cross sections are small. Compared to other analysis results[12], experimental cross section values are too small. The shape of angular distributions of analyzing power are generally well produced.

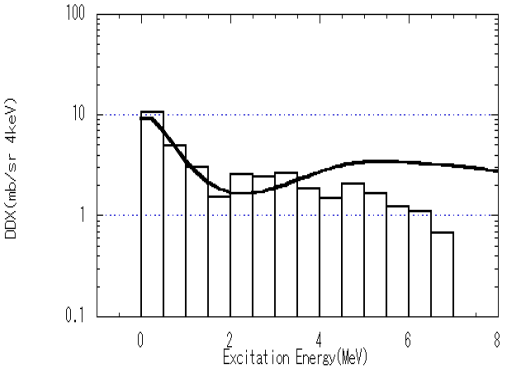

Figure 2: Comparison of theoretical and experimental double di®erential cross section. ^{100}Mo(p,d)^{99}Mo reaction at 50 MeV, θ =8 °laboratory angle.

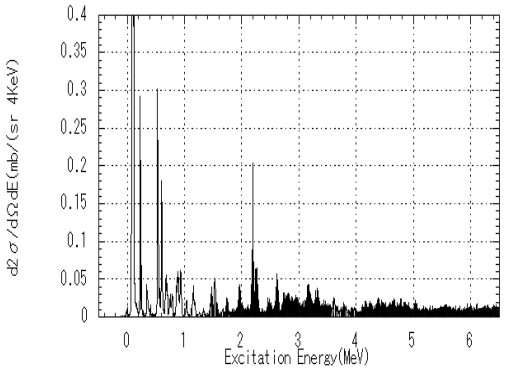

Figure 1: Typical energy spectrum of deuterons emitted from the ^{100}Mo(p,d)^{99}Mo reaction at 50 MeV.

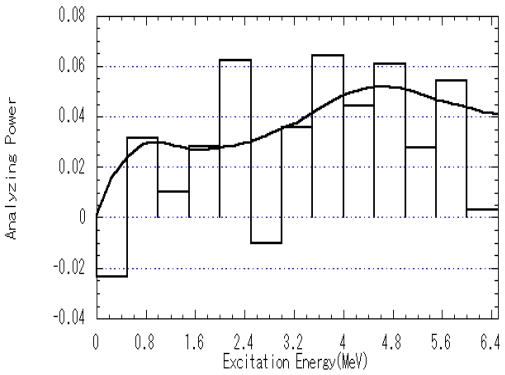

Figure 3: Comparison of theoretical and experimental danalyzing power. ^{100}Mo(p,d)^{99}Mo reaction at 50MeV, θ =8 °laboratory angle.

V. Conclusions

The use of a polized beam improved the results of spin parity assignments. Several new assignments are added to the previous results, especially in the relatively high excitation energy region (3～4MeV). Overall predictions of angular distributions are in good agreement with exprimental data for analyzing power distribution. This analysis gives a new possibility to distribution pattern of the continuum spectra for large scope of nuclei.

We are greateful to the staff of RCNP,Osaka University for their supports during the experiment.

References

[1] S.Hirowatari, Syafarudin, F.Aramaki, A.Nohtomi, G.Wakabayashi, Y.Uozumi, N.Ikeda, M.Matoba, Y.Aoki, K.Hirota, N.Okumura, and T.Joh, Nucl. Phys. A714 (2003) 3

[2] Syafarudin, F.Aramaki, G.Wakabayashi, Y.Uozumi, N.Ikeda, M.Matoba, K.Yamaguchi, T.Sakae, N.Koori, and T.Maki, International Conference on Nuclear Data for Science and Technology(ND2001-conf. 8-11 October 2001); J. Nucl. Sci. Technol., supplement. 2,(2002) 377.

[3] P.K.Bindal, D.H.Youngblood, R.L.Kozub, and P.H.Hoffmann-Pinther, Phys. Rev. C12 (1975) 1826.

[4] M.B.Lewis, Phys. Rev. C11(1975) 145.

[5] M.Matoba, O.Iwamoto, T.Sakae, N.Koori, H.Ohgaki, H.Kugimiya, H.Ijiri, T.Maki, and M.Nakano, Nucl. Phys. A581 (1995) 21.

[6] M.Matoba, K.Kuromaru, O.Iwamoto, A.Nohtomi, Y.Uozumi, T.Sakae, N.Koori, H.Ohgaki, H.Ijiri, T.Maki, M.Nakano, and H.M.Sen Gupta, Phys. Rev. C53 (1996) 1792.

[7] M.Matoba, O.Iwamoto, Y.Uozumi, T.Sakae, N.Koori, H.Ohgaki, H.Kugimiya, H.Ijiri, T.Maki, and M.Nakano, Nucl. Phys. A581 (1995) 21.

[8] C.Mahaux and R.Sartor, Nucl. Phys. A528 (1991) 253.

[9] G.E.Brown and M.Rho, Nucl. Phys. A372 (1981) 397.

[10] H.Langevin-Joliot, J.van de Wiele, J.Guillot, E.Gerlic, L.H.Rosier, A.Willis, M.Morlet, G.Duhamel-Chretien, E.Tomasi-Gustafsson, N.Blasi, S.Micheletti, and S.Y.van der Werf, Phys. Rev. C47 (1993) 1571

[11] P.D.Kunz, code DWUCK, University of Colorado (unpublished)

[12] R.B.Firestone, V.S.Shirley, C.M.Baglin, S.Y.Frank Chu, and J.Zipkin, Table of Isotopes 8th ed., New York, John Wiley (1996)

Table 1: Spectroscopic results from neutron pickup reactions on ^{100}Mo.

Present work				Ref.[3]					Ref.[12]	
E_x (MeV)	l	j^π	C^2S (p,d)	E_x (MeV)	l	j^π	C^2S (p,d)	(d,t)	E_x (MeV)	j^π
0.000	0	$\frac{1}{2}^+$	0.202	0.000	0	$\frac{1}{2}^+$	(0.30)	0.14	0.000	$\frac{1}{2}^+$
0.096	2	$\frac{5}{2}^+$	1.691	0.098	2	$\frac{5}{2}^+$	1.84	1.80	0.098	$\frac{5}{2}^+$
0.235	4	$\frac{7}{2}^+$	1.358	0.231	4	$\frac{7}{2}^+$	1.39	1.75	0.236	$\frac{7}{2}^+$
0.352	2	$\frac{3}{2}^+$	0.082	0.345	2	$\frac{3}{2}^+$	0.06	0.16	0.351	$\frac{3}{2}^+$
0.525	0	$\frac{1}{2}^+$	0.680	0.531	0	$\frac{1}{2}^+$			0.525	$\frac{1}{2}^+$
0.547	2	$\frac{5}{2}^+$	0.253		2	$\frac{3}{2}^+$	0.33	0.55	0.547	$\frac{3}{2}^+$
0.610	2	$\frac{5}{2}^+$	(0.253)	0.604	2	$\frac{5}{2}^+$	0.24	0.32	0.615	$\frac{5}{2}^+$
0.683	5	$\frac{11}{2}^-$	0.705	0.675	5	$\frac{11}{2}^-$	0.50	(1.20)	0.698	$(\frac{7}{2}^+)$
0.750	4	$\frac{7}{2}^+$	0.237	0.747	2	$\frac{5}{2}^+$	0.07	0.10	0.754	$\frac{7}{2}^+$
0.790	2	$\frac{3}{2}^+$	0.070	0.788	(2)	$(\frac{3}{2}^+)$	0.06	0.08	0.793	$(\frac{3}{2},\frac{5}{2})^+$
				0.878	(2)	$(\frac{3}{2}^+)$	0.07	0.06	0.890	$\frac{3}{2}^+$
0.897	4	$\frac{9}{2}^+$	0.412		(4)	$(\frac{9}{2}^+)$	0.59	0.30	0.906	$\frac{1}{2}^+$
0.938	2	$\frac{5}{2}^+$	0.131	0.924	2	$\frac{5}{2}^+$	0.15	0.22	0.945	$\frac{5}{2}^+$
1.037	3	$\frac{5}{2}^-$	0.205	1.022	(3)	$(\frac{5}{2}^-)$	0.26		1.026	$(\frac{3}{2}^+,\frac{5}{2}^+)$
1.157	2	$\frac{5}{2}^+$	0.125	1.165	2	$\frac{5}{2}^+$	0.10	0.08	1.167	$\frac{5}{2}^+$
1.262	0	$\frac{1}{2}^+$	0.041						1.280	
1.337	4	$\frac{7}{2}^+$	0.121	1.320	4	$\frac{7}{2}^+$	0.10			
1.471	2	$\frac{5}{2}^+$	0.084	1.455	2	$\frac{3}{2}^+$	0.10	0.10	1.494	$\frac{5}{2}^+$
1.532	2	$\frac{3}{2}^+$	0.129	1.516	2	$\frac{3}{2}^+$	0.13	0.15	1.561	$\frac{1}{2}^+,\frac{3}{2},\frac{5}{2}^+$
1.575	2	$\frac{3}{2}^+$	0.042						1.571	$\frac{1}{2},\frac{3}{2},\frac{5}{2}^+$
1.674	5	$\frac{11}{2}^-$	0.155	1.637	5	$\frac{11}{2}^-$	0.07			
									1.682	$(\frac{3}{2}^+,\frac{5}{2}^+)$
1.749	2	$\frac{5}{2}^+$	0.063	1.714	2	$\frac{3}{2}^+$	0.05	0.05		
				1.793	4	$\frac{7}{2}^+$	0.17	0.10		
1.847	5	$\frac{11}{2}^-$	0.156	1.891	1	$\frac{1}{2}^-$	0.12	0.11	1.893	$(\frac{1}{2}^-,\frac{3}{2}^-)$
1.967	1	$\frac{1}{2}^-$	0.201	1.910	1	$\frac{1}{2}^-$	0.27			
				1.934	4	$\frac{9}{2}^+$	0.19			
2.020										
2.119	4	$\frac{9}{2}^+$	0.844	2.103	4	$\frac{9}{2}^+$	1.02	1.00		
2.260	1	$\frac{1}{2}^-$	0.294	2.155	1	$\frac{1}{2}^-$	0.28	0.26		
2.383	1	$\frac{3}{2}^-$	0.062	2.330	2	$\frac{3}{2}^+$	0.063	1.00		
2.481				2.436	1	$\frac{1}{2}^-$	0.24	0.20		
				2.531	1	$\frac{1}{2}^-$	0.10			
2.622	1	$\frac{3}{2}^-$	0.252	2.591	1	$\frac{1}{2}^-$	0.09			
2.741	1	$\frac{1}{2}^-$	0.080	2.632	1	$\frac{1}{2}^-$	0.13			
2.820	1	$\frac{1}{2}^-$		2.702	1	$\frac{1}{2}^-$	0.10			
2.887	2	$\frac{3}{2}^+$	0.111	2.797	2	$\frac{5}{2}^+$	0.04			
2.970	2	$\frac{3}{2}^+$	0.120	2.870	1	$\frac{1}{2}^-$	0.17			
3.062	1	$(\frac{3}{2}^-)$	0.134							
3.170	2	$\frac{3}{2}^+$	0.221							
3.326	1	$\frac{3}{2}^-$	0.251							
3.497	4	$(\frac{7}{2}^+,\frac{9}{2}^+)$	0.251							
3.622	3	$\frac{7}{2}^+$	0.959							
3.731	2	$\frac{3}{2}^+$	0.078							
3.812	2	$\frac{3}{2}^+$	0.117							
4.174	1	$(\frac{3}{2}^-)$								